

Comparing allosteric transitions in the domains of calmodulin through coarse-grained simulations

Prithviraj Nandigrami and John J. Portman¹

Department of Physics, Kent State University, Kent, OH 44242

(Dated: 15 June 2021)

Calmodulin (CaM) is a ubiquitous Ca^{2+} -binding protein consisting of two structurally similar domains with distinct stabilities, binding affinities, and flexibilities. We present coarse grained simulations that suggest the mechanism for the domain's allosteric transitions between the open and closed conformations depend on subtle differences in the folded state topology of the two domains. Throughout a wide temperature range, the simulated transition mechanism of the N-terminal domain (nCaM) follows a two-state transition mechanism while domain opening in the C-terminal domain (cCaM) involves unfolding and refolding of the tertiary structure. The appearance of the unfolded intermediate occurs at a higher temperature in nCaM than it does in cCaM consistent with nCaM's higher thermal stability. Under approximate physiological conditions, the simulated unfolded state population of cCaM accounts for 10% of the population with nearly all of the sampled transitions (approximately 95%) unfolding and refolding during the conformational change. Transient unfolding significantly slows the domain opening and closing rates of cCaM. This potentially influences the mechanism of Ca^{2+} -binding to each domain.

INTRODUCTION

Allostery is central to the precise molecular control necessary for protein function. Indirect coupling between distant regions of a protein is often provided through a conformational transition between a “closed” (ligand-free) and “open” (ligand-bound) structure upon ligation. NMR experiments that reveal proteins exist in dynamic equilibrium with multiple conformers¹⁻⁶ suggest that a protein’s conformational dynamics in the absence of a ligand plays an essential role in allosteric regulation.⁷⁻¹⁰ The functional dynamics of a folded protein occurs near the bottom of the funneled energy landscape, a part of the landscape generally more susceptible to perturbations than the self-averaged kinetic bottleneck that determines the mechanism of folding.¹¹ This sensitivity, while important for a protein’s ability to dynamically respond to environmental conditions and interaction with ligands, also makes the prospect of general organizing principles for allostery problematic.¹² In this paper, we explore the sense in which the summarizing statement that native state topology determines the folding mechanism of small single domain proteins¹³ carries over to large-scale conformational transitions.

Due in part to limitations on computational timescales, much theoretical work modeling largescale conformational transitions in proteins has focused on simplified, coarse-grained models based on the energy basins defined by the open and closed conformations. The Gaussian network and related models describe an allosteric transition as motion along low frequency normal modes of the closed state conformational basin.¹⁴⁻¹⁷ While the dynamics about a single free energy minimum offers a natural rationale and clear description of the collective motions involved in the conformational change,^{18,19} a minimal model capable of capturing the transition mechanism must accommodate the change in dynamics as protein moves between the two distinct meta-stable free energy basins. Allosteric transitions have been modeled by several different methods in which two meta-stable basins are coupled through an interpolation based on its energy. For example, minimal energy pathways have been computed for a potential surface based on the strain energies relative to each minimum conformation to predict the transition mechanism.²⁰⁻²² Structure based simulations that couple two conformational basins have also been developed to understand the mechanism of allosteric transitions.²³⁻²⁸ Additionally, transition mechanisms have been described in terms of the evolution of each residue’s local flexibility using a coarse grained variational

model.²⁹⁻³² Itoh and Sasai present an alternative approach to predict allosteric transition mechanisms in which contacts from two meta-stable structures are treated on equal footing rather than through an interpolated energy function.^{33,34}

In this paper, we use coupled structure based simulation of the opening transition in the domains of calmodulin (CaM) to explore how subtle differences in the native state topology can lead to qualitative changes in the transition mechanism. This work is motivated in part by an intriguing theoretical prediction³⁰ that the domain opening mechanism of the C-terminal domain (cCaM) involves local partial unfolding and refolding while the N-terminal domain (nCaM) remains folded throughout the transition. These distinct transition mechanisms are in harmony with the Itoh and Sasai’s model that predicts cCaM has larger fluctuations than nCaM during domain opening.³⁴ Local unfolding in cCaM is found to relieve regions of high local strain during the transition³¹ in agreement with the cracking mechanism of allosteric transitions discussed by Miyashita et al.^{35,36}

CaM is a ubiquitous Ca^{2+} -binding protein consisting of two structurally similar globular domains connected by a flexible linker. Each domain consists of two helix-loop-helix motifs (the EF-hands) connected by a flexible linker as shown in Fig.1. Although topologically similar, the two CaM domains have distinct flexibilities, melting temperatures and thermodynamic Ca^{2+} -binding properties.³⁷⁻⁴⁰ In the absence of Ca^{2+} , the C-terminal domain is particularly dynamic⁴¹ and is less stable than the N-terminal domain in the intact protein and when separated into isolated domains.^{39,40,42} The C-terminal domain, which has a very low denaturation temperature, is reported to be considerably unfolded under physiological temperature.⁴³ Furthermore, NMR experiments monitoring the open/closed transition of isolated cCaM have revealed local transient unfolding of helix F during domain opening.⁴⁴

The simulations presented in this paper suggest that over a wide range of temperatures, domain opening in cCaM involves global unfolding and refolding, while the unfolded conformations are much less prominent in nCaM’s primarily two-state domain opening mechanism. The appearance of an unfolded intermediate at a sufficiently high temperature is expected and has been reported for similar simulations of the conformational transition of cCaM²⁶ and the homologous protein S100A6,²⁴ as well as other proteins.^{23,28} Given the structural similarity of the two domains, it is harder to anticipate that the unfolded ensemble becomes locally stable at a significantly higher temperature in nCaM than it does in cCaM. Both the analytic model and simulations suggest that cCaM is more susceptible to unfolding during

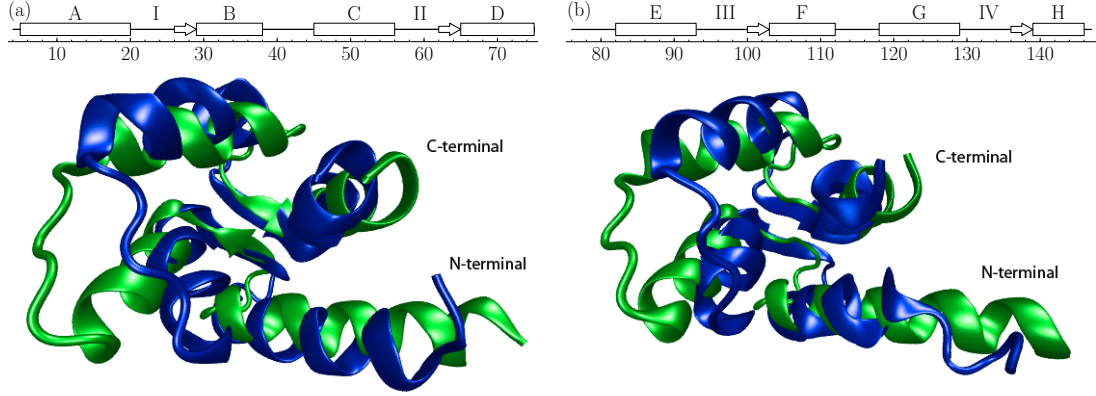


FIG. 1. Aligned structures Ca^{2+} -free (closed/apo) and Ca^{2+} -bound (open/holo) native conformations for (a) N-terminal domain and (b) C-terminal domain of Calmodulin. The closed state (pdb: 1cfd⁴⁶) is shown in blue, and the open state (pdb: 1cll⁴⁷) is shown in green. The closed (apo) and open (holo) conformations of (a) nCaM (residue index 4–75) consist of helices A, B and C, D with binding loops I and II respectively. The closed (apo) and open (holo) conformations of (b) cCaM (residue index 76–147) consist of helices E, F and G, H with binding loops III and IV respectively. Secondary structure legend for nCaM and cCaM are shown on top of the protein structures. The CaM structures were made using visual molecular dynamics.⁴⁸

domain opening, despite employing very different approximations. Nevertheless, the simulated intermediate is globally unfolded in contrast to the local unfolding predicted by the analytic model. In terms of the kinetics, global unfolding and refolding significantly slows the simulated domain opening rate in cCaM which potentially can bias the partitioning of Ca^{2+} -binding kinetics between induced fit and conformational selection for the two domains.

METHODS

We use a native-centric model implemented in the *Cafemol* simulation package⁴⁵ to study the open/closed conformational transitions of the isolated N-terminal and C-terminal domains of CaM. This model couples two energy basins, one biased to the open (holo) conformation and the other to the closed (apo) reference conformation.²⁴ The open and closed conformations of the domains of CaM are shown in Fig.1.

A conformation in this coarse-grained model²⁴ is specified by the N position vectors of the C- α atoms of the protein backbone, $\mathbf{R} = \{\mathbf{r}_1, \dots, \mathbf{r}_N\}$. For an energy basin biased to the

reference conformation, \mathbf{R}_0 , the energy of a configuration \mathbf{R} can be written as

$$V_0(\mathbf{R}) = V_{\text{local}}(\mathbf{R}|\mathbf{R}_0) + V_{\text{n}}(\mathbf{R}|\mathbf{R}_0) + V_{\text{nn}}(\mathbf{R}|\mathbf{R}_0). \quad (1)$$

The first term in Eq. 1 defines the coarse-grained backbone

$$\begin{aligned} V_{\text{local}}(\mathbf{R}|\mathbf{R}_0) = & \sum_{\text{bonds}} K_b (b_i - b_i^0)^2 + \sum_{\text{angles}} K_\theta (\theta_i - \theta_i^0)^2 \\ & + \sum_{\text{dihedrals}} [K_\phi [1 - \cos(\phi_i - \phi_i^0)] \\ & + K_\phi^{(3)} [1 - \cos 3(\phi_i - \phi_i^0)]] , \end{aligned} \quad (2)$$

where b_i , θ_i , and ϕ_i denote bond lengths, bond angles, and dihedral angles, respectively. The corresponding values in the native structure are denoted with a superscript: b_i^0 , θ_i^0 , and ϕ_i^0 . The non-bonded interaction between neighboring residues in the native structure (native contacts) have short-ranged attraction

$$V_{\text{n}}(\mathbf{R}|\mathbf{R}_0) = \sum_{\substack{i < j - 3 \\ \text{native} \\ \text{contacts}}} \epsilon_{\text{go}} \left[5 \left(\frac{r_{ij}^0}{r_{ij}} \right)^{12} - 6 \left(\frac{r_{ij}^0}{r_{ij}} \right)^{10} \right], \quad (3)$$

while non-native contacts are destabilized through a repulsive potential

$$V_{\text{nn}}(\mathbf{R}|\mathbf{R}_0) = \sum_{\substack{i < j - 3 \\ \text{non-native}}} \epsilon_{\text{rep}} \left(\frac{d}{r_{ij}} \right)^{10}. \quad (4)$$

Here, r_{ij} is the distance between C- α atoms i and j in a conformation, \mathbf{R} , and r_{ij}^0 is the corresponding separation distance found in the reference structure, \mathbf{R}_0 .

The coefficients defining the energy function are set to their default values in *Cafemol*: $K_b = 100.0$, $K_\theta = 20.0$, $K_\phi^{(1)} = 1.0$ and $K_\phi^{(3)} = 0.5$, $\epsilon_{\text{go}} = 0.3$, $\epsilon_{\text{rep}} = 0.2$ in units of kcal/mol, and $d = 4\text{\AA}$. Trajectories are simulated using Langevin dynamics with a friction coefficient of $\gamma = 0.25$ and a timestep of $\Delta t = 0.2$ (in coarse-grained units).²⁵ With these parameters, the folding transition temperatures of the isolated CaM domains are estimated from equilibrium trajectories to be $T_{\text{F}}^{\text{o}}(\text{nCaM}) = 333.6^\circ\text{K}$ and $T_{\text{F}}^{\text{c}}(\text{nCaM}) = 328.9^\circ\text{K}$ for the open and closed state of nCaM, and $T_{\text{F}}^{\text{o}}(\text{cCaM}) = 335.1^\circ\text{K}$ and $T_{\text{F}}^{\text{c}}(\text{cCaM}) = 330.5^\circ\text{K}$ for the open and closed state of cCaM, respectively. Experimentally, the isolated domains have similar folding

transition temperatures of approximately 323°K ⁴⁰. Although $T_F^o(\text{cCaM})$ and $T_F^o(\text{nCaM})$ as well as $T_F^c(\text{cCaM})$ and $T_F^c(\text{nCaM})$ are within 2°K (with cCaM’s thermal stability slightly below nCaM’s), coupling the open and closed basins significantly destabilizes cCaM with respect to nCaM (described below). Consequently, the simulations relevant to the domains of intact CaM, for which interactions between the domains, particularly with the linker region⁴⁹, reduce the folding temperature of the C-terminal domain to roughly 315°K and increase the folding temperature of N-terminal domain to 328°K .^{37,39,40}

To study conformational changes between two meta-stable states, the energies of the corresponding native basins, $V_1(\mathbf{R})$ and $V_2(\mathbf{R})$, are coupled through an interpolation function⁴⁵

$$V(\mathbf{R}) = \frac{V_1 + V_2 + \Delta V}{2} - \sqrt{\left(\frac{V_1 - V_2 - \Delta V}{2}\right)^2 + \Delta^2}. \quad (5)$$

Here, the interpolation parameters, Δ and ΔV , control the barrier height and the relative stability of the two basins. The single basin energies $V_1(\mathbf{R})$ and $V_2(\mathbf{R})$ are computed from Eq. 1 with modifications to some of the reference parameters in the potential in order to minimize conflicts between the two contact maps. (See Ref. 24, 25, and 45 for details).

To compare the simulated domain opening mechanisms most clearly, it is convenient to choose coupling parameters Δ and ΔV so that the barrier between the two states is low enough to give sufficient sampling of the two states and equal stability of the open and closed conformations (a choice to improve sampling of the equilibrium transition kinetics). With $\Delta = 14.0 \text{ kcal/mol}$ and $\Delta V = 2.15 \text{ kcal/mol}$ for nCaM, and $\Delta = 17.5 \text{ kcal/mol}$ and $\Delta V = 0.25 \text{ kcal/mol}$ for cCaM, the open and closed states are equally probable with a free energy barrier of $\simeq 4k_B T$ as shown in Fig.2. With these parameters, the folding temperature for cCaM is approximately 25 degrees below the folding temperature of nCaM as indicated by the peaks in the heat capacity shown in Fig.3. We report temperatures relative to the simulated folding temperature of cCaM, denoted as $T_F^* = 275.0^\circ\text{K}$. Although we have explored a wide range of temperatures, most of the results presented in this paper have $T_{\text{sim}} = 0.96T_F^*$, a temperature slightly below the folding temperature of cCaM, and significantly below the folding temperature of nCaM.

NMR experiments indicate that the closed state of cCaM is more stable than the open state under physiological conditions, accounting for roughly 90% of the population.⁵⁰ Assuming nCaM is similar, we adjust the relative stability of both domains through the coupling parameter ΔV to match this stability ($\Delta V = 3.5 \text{ kcal/mol}$ for nCaM, and $\Delta V = 4.0 \text{ kcal/mol}$

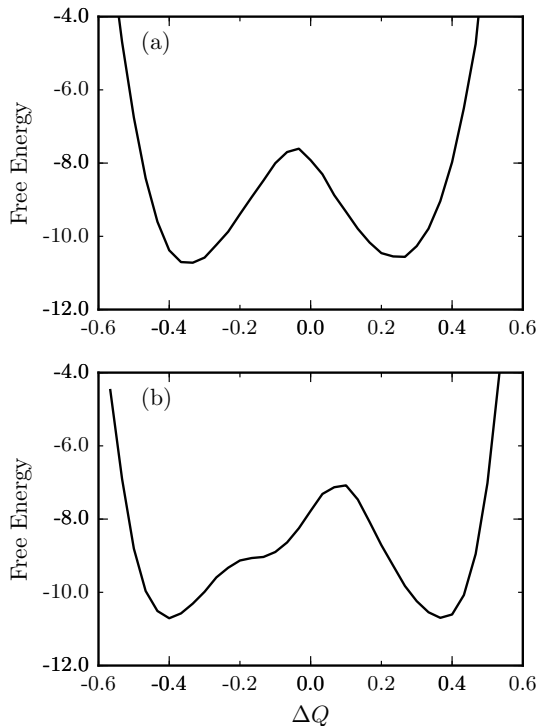


FIG. 2. Simulated free energy (in units of $k_B T$) as a function of the global progress coordinate $\Delta Q = Q_{\text{closed}} - Q_{\text{open}}$ for (a) nCaM and (b) cCaM.

for cCaM). As shown in Fig.3, the folding temperatures of the domains are sensitive to this destabilization of the open state. The simulated folding temperatures of the two domains differ by approximately 18°K , somewhat larger than the difference in experimental folding temperatures of the domains in intact CaM, approximately 13°K .⁴³ To connect to the domain opening kinetics in intact CaM, we relate the simulated temperatures to the folding temperatures of its N-terminal and C-terminal domains. With this choice, the physiological temperature 310°K corresponds to simulation temperature of 95% of nCaM's folding temperature, and 98% of cCaM's folding temperature.

Simulated conformational ensembles are characterized through local and global structural order parameters based on the contacts formed in each sampled conformation. A native contact is considered to be formed if the distance between the residues is closer than 1.2 times the corresponding distance in the native conformation. To characterize structural changes during the conformational transition, it is convenient to separate the set of native contacts in the open (holo) and closed (apo) conformations into three groups: those that

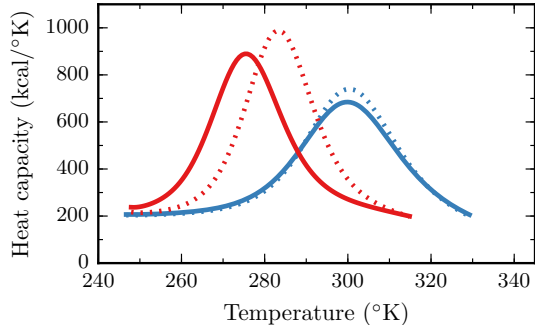


FIG. 3. Heat capacity as a function of temperature for cCaM (red) and nCaM (blue) for two relative stabilities of the open and closed basins. The solid curves correspond to equally stable open and closed basins, and in the dashed curves the open state occupies approximately 10% of the total population.

occur exclusively in either the open or the closed native reference conformation, and those that are common to both states. For each of these groups, denoted by $\alpha = (\text{open}, \text{closed}, \text{and } \cap)$, we define a local order parameter, $q_\alpha(i)$, as the fraction of native contacts formed involving the i^{th} residue. Overall native similarity is monitored by corresponding global order parameters, $Q_\alpha = \langle q_\alpha(i) \rangle$, where the average is taken over the residues of the protein. The free energy parameterized by these global order parameters are used to identify locally stable conformational ensembles such as the open and closed basins.

The transition rates between two coarse-grained ensembles are calculated from equilibrium simulations of length 10^8 steps typically involving $O(10^3)$ open/closed transitions for nCaM and $O(10^2)$ open/closed transitions for cCaM. The transition rate between two states labeled by i and j is estimated by⁵¹

$$k_{i \rightarrow j} = \frac{N_{i \rightarrow j}}{\langle \tau_i \rangle \sum_{k \neq i} N_{i \rightarrow k}}, \quad (6)$$

where $\langle \tau_i \rangle$ is the mean time spent in state i between transitions, and $N_{i \rightarrow j}$ are the number of transitions from state i to state j . When the allosteric transition involves only the open and closed states, Eq. 6 reduces to the two state rates, $k_{o \rightarrow c} = \langle \tau_o \rangle^{-1}$ and $k_{c \rightarrow o} = \langle \tau_c \rangle^{-1}$, where $\langle \tau_o \rangle$ and $\langle \tau_c \rangle$ are the mean first passage times to leave the open and closed state, respectively.

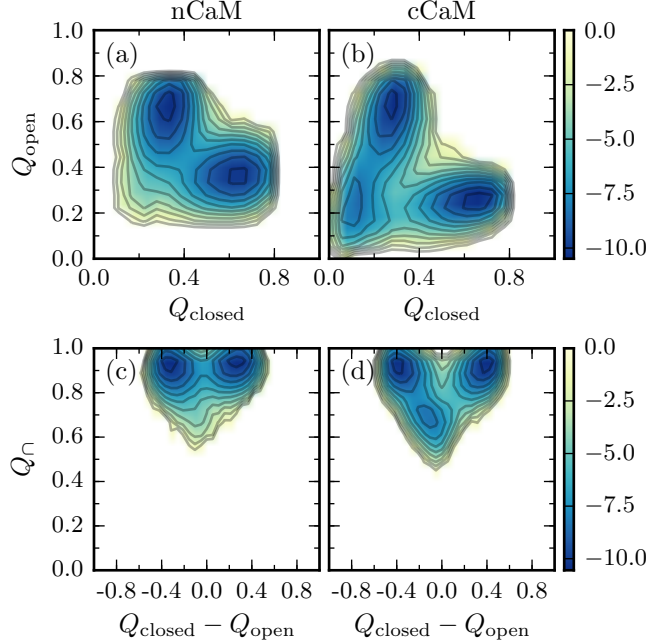


FIG. 4. Free energy, in units of $k_B T$, projected onto global order parameters Q_{open} , Q_{closed} , and Q_{\cap} for nCaM (a and c) and cCaM (b and d). The intermediate in free energy surface of cCaM corresponds to an ensemble of states with intact secondary structure but lacking stable tertiary contacts.

CONFORMATIONAL TRANSITIONS OF ISOLATED DOMAINS

The populations of simulated conformations organized in terms of global order parameters are shown in Fig.4. The free energy as a function of Q_{open} and Q_{closed} shows that the nCaM has a two-state domain opening and its conformational transition is sequential. That is, contacts specific to the closed conformation are lost prior to formation of contacts specific to the open conformation which mostly form after transition state region. Fig.4 also shows the free energy projected onto the order parameter monitoring common contacts, Q_{\cap} , and a progress coordinate for the conformational transition, $\Delta Q = Q_{\text{closed}} - Q_{\text{open}}$. The global order parameter Q_{\cap} monitors the overall structural integrity of the secondary structure as well as tertiary contacts within parts of the protein that do not have large conformational changes during the transition. As shown in Fig.4, the common contacts in nCaM's transition state ensemble remain largely intact. In contrast, the simulated open/closed free energy for cCaM has a locally stable intermediate state. Simultaneously low values of Q_{open} and Q_{closed}

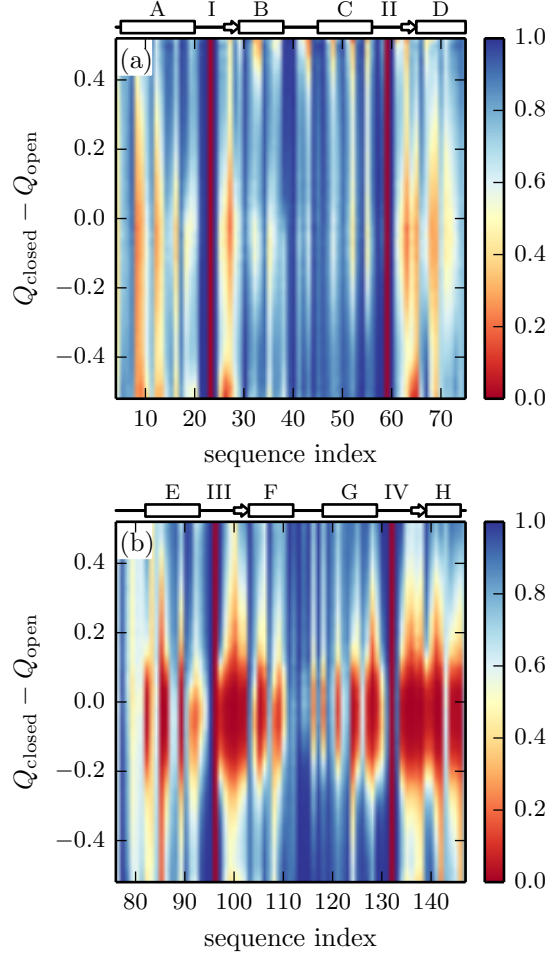


FIG. 5. Local order parameter, $q_{\cap}(i)$, plotted as a function of the global progress coordinate, $Q_{\text{closed}} - Q_{\text{open}}$, for each residue of (a) nCaM and (b) cCaM. The color represents the probability of each residue forming native contacts common to both the open and closed structures: low probability is shown by red and high probability is shown by blue.

(both less than 0.3), and Q_{\cap} (less than 0.7), indicate that the intermediate has significantly reduced tertiary structure. The probability to form individual contacts in the intermediate (data not shown) verifies that the secondary structure remains intact, though nearly all the tertiary interactions are lost. Since the barrier for the transition closed \rightarrow I ($\Delta F^{\ddagger} \simeq 4 \text{ k}_B\text{T}$) is higher than the barrier for I \rightarrow open ($\Delta F^{\ddagger} \simeq 1.5 \text{ k}_B\text{T}$), the intermediate can be considered to be part of cCaM's extended open basin.

To describe the transition mechanism at the residue level, we consider the local order parameter $q_{\cap}(i)$ of each residue as a function of the global progress coordinate ΔQ . As

shown in Fig.5, cCaM’s residues lose the majority of their common contacts upon opening (moving upward in the plot) and regain them later in the transition. Although the folding and refolding of residues in helices E and H are more gradual than other residues, nearly every residue (except the residues in the linker region between helices F and G) loses native tertiary structure. In contrast, the common contacts in nCaM remain intact throughout the transition, though the contacts involving specific residues in helices A and D and the β -sheets in the loops are strained. Limited loss of long range common contacts in nCaM reflect an increased flexibility of the folded transition state ensemble.

A coarse-grained, analytic model, also predicts distinct transition mechanisms for each domain in which cCaM is susceptible to local unfolding during the open/closed transition, while nCaM remains folded.^{30,31} The conformational transition in the analytic model is described as the evolution of local flexibility along the transition route. Fig.6 shows the simulated local flexibility for four discrete values of the progress coordinate, ΔQ . Although the fluctuations of the residues in both domains increase and then decrease during the transition, the magnitude of the largest fluctuations are much greater in cCaM. In contrast to the global unfolding observed in the simulations, unfolding and refolding of cCaM predicted by the analytic model is localized to particular residues (primarily in the linker between helix F and G).

Exploring a range of temperatures reveals that both domains can exhibit a two-state transition mechanism or a transition mechanism that involves unfolding and refolding depending on the temperature (see Fig.7). The transition mechanism at low temperatures is two state, involving primarily well folded conformational ensembles throughout the transition. Increasing the temperature progressively stabilizes the unfolded ensemble until it becomes locally stable at a spinodal temperature, T_s . Above the spinodal temperature, the transition between the open and closed state involves unfolding and refolding of the domain. At high enough temperatures, the unfolded conformation becomes the most stable state.

Although both domains follow similar transition scenarios as a function of temperature, the domains can have different transition mechanisms from each other because the spinodal temperatures are different. Comparing the two domains, cCaM has a lower spinodal temperature ($T_s^c \approx 0.93T_F^*$) than nCaM ($T_s^n \approx 1.005T_F^*$). For low temperatures, ($T < T_s^c$), both the domains have two state transitions. For intermediate temperatures ($T_s^c < T < T_s^n$), the domain opening transition of nCaM is two state, while the transition of cCaM involves

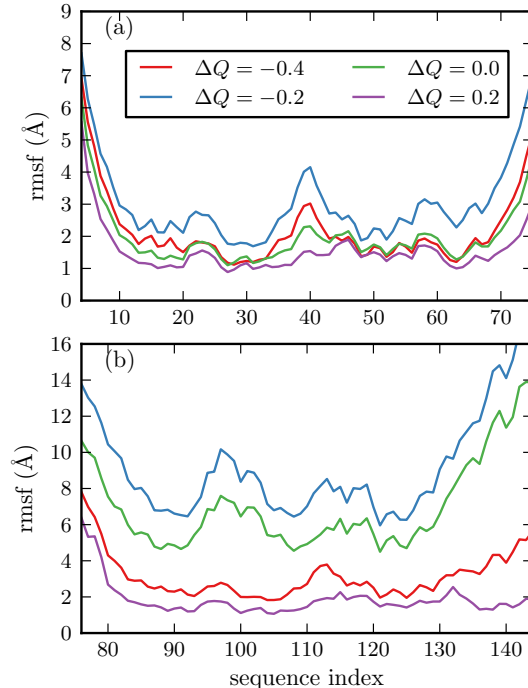


FIG. 6. Magnitude of the root mean square fluctuations for each residue for the conformational ensembles along the transition pathway for (a) nCaM and (b) cCaM. Each color corresponds to the value of $\Delta Q = Q_{\text{closed}} - Q_{\text{open}}$ indicated in the legend in (a).

unfolding and refolding. For higher temperatures ($T_s^n < T$), the unfolded ensemble of nCaM is locally stable, but at this temperature the unfolded ensemble of cCaM is stabilized enough to become the global minimum.

Focusing on the scenario when the open state is 10% of the total population and at a simulation temperature corresponding to $T = 310^\circ\text{K}$ (to model intact CaM at physiological conditions), the simulated unfolded population is less than 1% for nCaM, and approximately 9% for cCaM. These equilibrium unfolded populations can be compared to reports of 2% for the N-terminal domain and 24% for the C-terminal domain in intact CaM based on thermodynamic stability measurements.⁴⁰

TRANSITION KINETICS

Using Eq. 6 to calculate opening rates for each domain at T_{sim} , we find that unfolding and refolding along the transition route significantly slows cCaM's domain opening rate

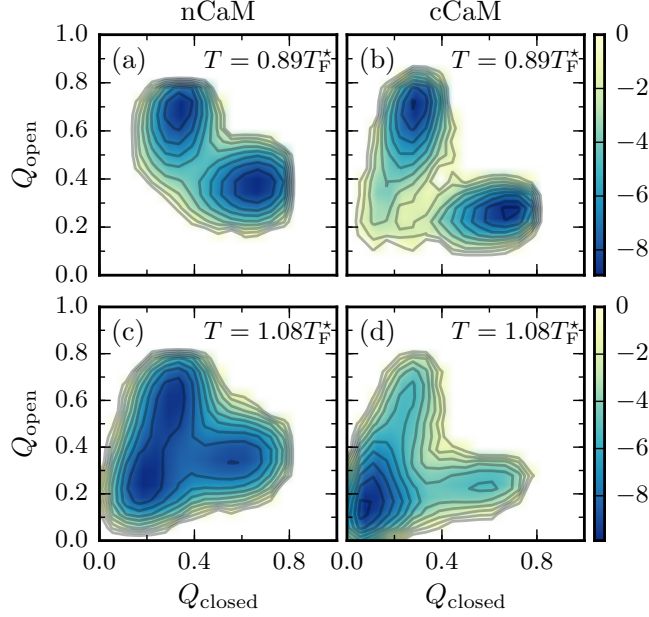


FIG. 7. Free energy, in units of $k_B T$, projected onto global order parameters Q_{closed} and Q_{open} for nCaM (a and c) and cCaM (b and d) with temperature $T_{\text{sim}} = 0.89T_F^*$ and $T_{\text{sim}} = 1.08T_F^*$. At lower temperatures, the unfolded conformations are destabilized so that the transition mechanism in both domains becomes more two-state. At higher temperatures, the unfolded states are stabilized for both nCaM and cCaM.

compared to nCaM. Quantitatively, the domain opening and closing rates of nCaM, $k_{o \rightarrow c} = k_{c \rightarrow o} = 2 \times 10^{-3} \Delta t^{-1}$, are 50 times larger than the effective opening and closing rates of cCaM, $k_{o \rightarrow c} = k_{c \rightarrow o} = 4 \times 10^{-5} \Delta t^{-1}$.

A closer look at cCaM's kinetic transitions reveals that only $\approx 5\%$ of its transition paths proceed through direct transitions from the closed to open state without significant unfolding along the way. The rest of the transitions occur according to the kinetic equation



where $k_{c \rightarrow I} = 4 \times 10^{-5} \Delta t^{-1}$, $k_{I \rightarrow c} = 2 \times 10^{-4} \Delta t^{-1}$, $k_{I \rightarrow o} = 8 \times 10^{-3} \Delta t^{-1}$, and $k_{o \rightarrow I} = 2 \times 10^{-3} \Delta t^{-1}$ are the corresponding simulated rates between the open, closed, and intermediate states.

Equilibrium between the open and the unfolded intermediate is established quickly on the timescale of the conformational transition so that the unfolded intermediate establishes

a steady-state population

$$P_I = \frac{k_{c \rightarrow I} P_c + k_{o \rightarrow I} P_o}{k_{I \rightarrow c} + k_{I \rightarrow o}}, \quad (8)$$

where P_c and P_o are the equilibrium populations of the closed and open state respectively.

The effective two-state kinetics for open/closed transition can be written as

$$k_{c \rightarrow o}^{\text{eff}} = \frac{k_{c \rightarrow I} k_{I \rightarrow o}}{k_{I \rightarrow c} + k_{I \rightarrow o}} \quad (9)$$

and

$$k_{o \rightarrow c}^{\text{eff}} = \frac{k_{o \rightarrow I} k_{I \rightarrow c}}{k_{I \rightarrow c} + k_{I \rightarrow o}}. \quad (10)$$

Since $k_{I \rightarrow c} \ll k_{I \rightarrow o}$, these expressions for the two-state rates can be simplified. The effective domain opening rate is determined by the unfolding of the closed state

$$k_{c \rightarrow o}^{\text{eff}} \approx k_{c \rightarrow I}, \quad (11)$$

and the closing rate can be understood through the equilibration of the intermediate and open state

$$k_{o \rightarrow c}^{\text{eff}} \approx k_{I \rightarrow c} \left(\frac{P_I}{P_o} \right), \quad (12)$$

where $P_I/P_o = 0.2$ is the population of the unfolded intermediate relative to the open state. The simulated effective two state rates for cCaM are consistent with this steady-state description of the kinetics.

The slowing influence of the folding and unfolding transition persists when the open state is destabilized to 10% of the total population, with domain opening approximately 45 times faster in nCaM than in cCaM at simulated temperatures that correspond to $T = 310^\circ\text{K}$.

DISCUSSION

Although the isolated domains of CaM are topologically similar, the simulated open/closed transition mechanisms are distinct due to the presence of an unfolded intermediate that appears in the free energy landscape at a different temperature for each domain. Two-state transition kinetics persist at higher temperatures in nCaM, whereas the unfolded ensemble is more readily stabilized in cCaM. Above the spinodal temperature, transient unfolding and refolding of the domain occurs through the locally stable unfolded intermediate (exemplified by cCaM at T_{sim}). Below the spinodal temperature, the transition is two-state like

albeit with conformational dynamics that anticipates the unfolded intermediate with high flexibility and stressed tertiary interactions (as in nCaM at T_{sim}).

The unfolding and refolding along the open and closed transition is reminiscent of the cracking mechanism^{35,36,52} in which regions of high local strain are relieved through unfolding and refolding in the transition region. Since the unfolded conformations involved in cracking are typically locally unstable, the domain opening of CaM most closely follows this canonical description at temperatures near the spinodal for the unfolded conformations.

High temperature unfolded intermediates have been reported previously in simulations of the open/closed transition in cCaM²⁶ and the homologous protein S100A6.²⁴ Chen and Hummer found that the population of the open ensemble is comparable to that of a marginally stable unfolded ensemble within a narrow temperature range. They argue that the sensitive balance between unstable folding and unfolded populations explains why some experiments report an open/closed transition,^{3,44,50,53,54} and others report folding/unfolding transition for cCaM under similar conditions.⁴³

Our simulations suggest that subtle differences in the topology and stability of the two domains can result in distinct transition mechanisms. In particular, we find that the unfolded population is stabilized more readily in cCaM, a result consistent with the prediction that cCaM (and not nCaM) exhibits local folding and unfolding during opening.^{29,31} The C-terminal domain's lower spinodal temperature may reflect its decreased overall relative thermodynamic stability. Indeed, nCaM is measured to be more stable than cCaM in the absence of Ca^{2+} ,³⁹ with cCaM being significantly unfolded at room temperature (20 – 25°C).⁴⁰

The transient unfolding and refolding observed in the simulations significantly slows the transition kinetics of cCaM. Several key observations of CaM dynamics have been reported, but how the dynamics of the individual domains compare is not clear from the literature. NMR studies of intact CaM in the absence of Ca^{2+} report that cCaM is more dynamic than the nCaM, with an exchange time of 350 μs for cCaM.⁴¹ This timescale is comparable to the folding and unfolding equilibration time of 200 μs for cCaM under similar conditions.⁴³ The dynamics of Ca^{2+} -loaded cCaM with a mutation E140Q that stabilizes the open state and prevents binding to loop IV exhibits exchange on the faster timescale of 25 μs ⁴ and undergoes local transient unfolding.⁴⁴ The dynamics of both domains under similar conditions has been reported by Price and co-workers who used fluorescence correlation spectroscopy coupled to Förster Resonance Energy Transfer (FRET) to monitor the intramolecular dy-

namics of both nCaM and cCaM on the microsecond timescale.⁵⁵ They report that both domains have fluctuations on the 30 – 40 μ s timescale in the absence of Ca^{2+} . The Ca^{2+} -dependence of the fluctuation amplitude, however, indicates that the observed fluctuations couple to the occupancy of the binding sites (and hence to domain opening) only in nCaM. Taken together, the evidence that the two domains have a different conformational timescale and/or mechanism is intriguing in light of the predictions from the coarse-grained simulations. Nevertheless, understanding how flexibility and transient unfolding influences domain opening dynamics of CaM requires further experimental clarification.

CONCLUDING REMARKS

Understanding the open/closed conformational dynamics of CaM is an essential step towards modeling Ca^{2+} -binding. Exploring how transient unfolding in domain opening of CaM influences ligand binding is particularly interesting. Simulations of an extension of this model that includes Ca^{2+} -binding (reported in a separate publication) shows that the two domains differ significantly in their thermodynamic properties such as binding affinity and cooperativity. Nevertheless, these thermodynamic differences seem to depend on the distinct conformational properties of the open and closed ensembles of each domain rather than the presence of an unfolded intermediate. Transient unfolding may still influence binding kinetics due to the slowing of the domain opening rate. This is particularly interesting because the detailed binding mechanism, such as the partitioning of binding kinetics into conformational selected or induced fit binding routes⁵⁶ is thought to be sensitive to the timescale of the open and closed transition.⁵⁷ Clarifying how the speed of conformational dynamics influences the kinetic binding mechanism through a molecular model is a rich problem that we wish to explore in the future.

ACKNOWLEDGMENTS

We would like to thank Swarnendu Tripathi for interesting discussions, and Daniel Gavazzi for help in preparing some of the figures. Financial support from the National Science Foundation Grant No. MCB-0951039 is gratefully acknowledged.

REFERENCES

- ¹G. Barbato, M. Ikura, L. E. Kay, R. W. Pastor, and A. Bax, *Biochemistry* **31**, 5269 (1992).
- ²F. J. Moy, D. F. Lowry, P. Matsumura, F. W. Dahlquist, J. E. Krywko, and P. J. Dommelle, *Biochemistry* **33**, 10731 (1994).
- ³J. Evenäs, S. Forsén, A. Malmendal, and M. Akke, *J. Mol. Biol.* **289**, 603 (1999).
- ⁴J. Evenäs, A. Malmendal, and M. Akke, *Structure* **9**, 185 (2001).
- ⁵B. F. Volkman, D. Lipson, D. E. Wemmer, and D. Kern, *Science* **291**, 2429 (2001).
- ⁶K. A. Henzler-Wildman, V. Thai, M. Lei, M. Ott, M. Wolf-Watz, T. Fenn, E. Pozharski, M. A. Wilson, G. A. Petsko, M. Karplus, *et al.*, *Nature* **450**, 838 (2007).
- ⁷B. Ma, S. Kumar, C. J. Tsai, and R. Nussinov, *Protein Eng.* **12**, 713 (1999).
- ⁸J. F. Swain and L. M. Gierasch, *Current Opinion in Structural Biology* **16**, 102 (2006).
- ⁹K. Henzler-Wildman and D. Kern, *Nature* **450**, 964 (2007).
- ¹⁰D. D. Boehr, R. Nussinov, and P. E. Wright, *Nat. Chem. Biol.* **5**, 789 (2009).
- ¹¹J. D. Bryngelson, J. N. Onuchic, N. D. Socci, and P. G. Wolynes, *Proteins* **21**, 167 (1995).
- ¹²P. I. Zhuravlev and G. A. Papoian, *Quarterly Reviews of Biophysics* **43**, 295 (2010).
- ¹³D. Baker, *Nature* **405**, 39 (2000).
- ¹⁴I. Bahar, A. R. Atilgan, and B. Erman, *Folding and Design* **2**, 173 (1997).
- ¹⁵A. Atilgan, S. Durell, R. Jernigan, M. Demirel, O. Keskin, and I. Bahar, *Biophysical Journal* **80**, 505 (2001).
- ¹⁶F. Tama and Y. Sanejouand, *Protein Engineering Design and Selection* **14**, 1 (2001).
- ¹⁷I. Bahar and A. Rader, *Current Opinion in Structural Biology* **15**, 586 (2005).
- ¹⁸L. Yang, G. Song, and R. L. Jernigan, *Biophys. J.* **93**, 920 (2007).
- ¹⁹I. Bahar, T. R. Lezon, L. W. Yang, and E. Eyal, *Annual Review of Biophysics* **39**, 23 (2010).
- ²⁰P. Maragakis and M. Karplus, *J. Mol. Biol.* **352**, 807 (2005).
- ²¹J. Chu and G. Voth, *Biophys. J.* **93**, 3860 (2007).
- ²²A. Das, M. Gur, M. H. Cheng, S. Jo, I. Bahar, and B. Roux, *PLoS Comput. Biol.* **10**, e1003521 (2014).
- ²³R. B. Best, Y. G. Chen, and G. Hummer, *Structure* **13**, 1755 (2005).

- ²⁴K. Okazaki, N. Koga, S. Takada, J. N. Onuchic, and P. G. Wolynes, *Proc. Natl. Acad. Sci. U. S. A.* **103**, 11844 (2006).
- ²⁵K. Okazaki and S. Takada, *Proc. Natl. Acad. Sci. U. S. A.* **105**, 11182 (2008).
- ²⁶Y. G. Chen and G. Hummer, *J. Am. Chem. Soc.* **129**, 2414 (2007).
- ²⁷Q. Lu and J. Wang, *J. Am. Chem. Soc.* **130**, 4772 (2008).
- ²⁸S. Yang and B. Roux, *PLoS Comput. Biol.* **4**, e1000047 (2008).
- ²⁹S. Tripathi and J. J. Portman, *J. Chem. Phys.* **128**, 205104 (2008).
- ³⁰S. Tripathi and J. J. Portman, *Proc. Natl. Acad. Sci. U. S. A.* **106**, 2104 (2009).
- ³¹S. Tripathi and J. J. Portman, *J. Chem. Phys.* **135**, 075104 (2011).
- ³²S. Tripathi and J. J. Portman, *The Journal of Physical Chemistry B* **117**, 13182 (2013).
- ³³K. Itoh and M. Sasai, *Proc. Natl. Acad. Sci. U. S. A.* **107**, 7775 (2010).
- ³⁴K. Itoh and M. Sasai, *J. Chem. Phys.* **134**, 125102 (2011).
- ³⁵O. Miyashita, J. N. Onuchic, and P. G. Wolynes, *Proc. Natl. Acad. Sci. U. S. A.* **100**, 12570 (2003).
- ³⁶O. Miyashita, P. G. Wolynes, and J. N. Onuchic, *J. Phys. Chem. B* **109**, 1959 (2005).
- ³⁷T. N. Tsalkova and P. L. Privalov, *J. Mol. Biol.* **181**, 533 (1985).
- ³⁸S. Linse, A. Helmersson, and S. Forsen, *Journal of Biological Chemistry* **266**, 8050 (1991).
- ³⁹B. R. Sorensen and M. A. Shea, *Biochemistry* **37**, 4244 (1998).
- ⁴⁰L. Masino, S. R. Martin, and P. M. Bayley, *Protein Sci.* **9**, 1519 (2000).
- ⁴¹N. Tjandra, H. Kuboniwa, H. Ren, and A. Bax, *European Journal of Biochemistry* **230**, 1014 (1995).
- ⁴²J. P. Browne, M. Strom, S. R. Martin, and P. M. Bayley, *Biochemistry* **36**, 9550 (1997).
- ⁴³C. R. Rabl, S. R. Martin, E. Neumann, and P. M. Bayley, *Biophys. Chem.* **101-102**, 553 (2002).
- ⁴⁴P. Lundström, F. A. A. Mulder, and M. Akke, *Proc. Natl. Acad. Sci. U. S. A.* **102**, 16984 (2005).
- ⁴⁵H. Kozaki, N. Koga, N. Hori, R. Kanada, W. Li, K. Okazaki, X. Q. Yao, and S. Takada, *Journal of Chemical Theory and Computation* **7**, 1979 (2011).
- ⁴⁶H. Kuboniwa, N. Tjandra, S. Grzesiek, H. Ren, C. B. Klee, and A. Bax, *Nat. Struct. Biol.* **2**, 768 (1995).
- ⁴⁷R. Chattopadhyaya, W. E. Meador, A. R. Means, and F. A. Quiocho, *J. Mol. Biol.* **228**, 1177 (1992).

- ⁴⁸W. Humphrey, A. Dalke, and K. Schulten, *Journal of Molecular Graphics* **14**, 33 (1996).
- ⁴⁹S. E. O'Donnell, R. A. Newman, T. J. Witt, R. Hultman, J. R. Froehlig, A. P. Christensen, and M. A. Shea, *Methods in Enzymology* **466**, 503 (2009).
- ⁵⁰A. Malmendal, J. Evenäs, S. Forsén, and M. Akke, *J. Mol. Biol.* **293**, 883 (1999).
- ⁵¹N. Buchete and G. Hummer, *The Journal of Physical Chemistry B* **112**, 6057 (2008).
- ⁵²P. Whitford, O. Miyashita, Y. Levy, and J. N. Onuchic, *J. Mol. Biol.* **366**, 1661 (2007).
- ⁵³D. Vigil, S. C. Gallagher, J. Trehwella, and A. E. García, *Biophys. J.* **80**, 2082 (2001).
- ⁵⁴P. Lundström and M. Akke, *J. Am. Chem. Soc.* **126**, 928 (2004).
- ⁵⁵E. Price, M. Aleksiejew, and C. Johnson, *The Journal of Physical Chemistry B* (2011).
- ⁵⁶G. G. Hammes, Y. C. Chang, and T. G. Oas, *Proc. Natl. Acad. Sci. U. S. A.* **106**, 13737 (2009).
- ⁵⁷L. Cai and H. X. Zhou, *J. Chem. Phys.* **134**, 105101 (2011).